2018 European Control Conference (ECC)
June 12-15, 2018. Limassol, Cyprus

New approximate solution with resonance modes of Saint-Venant equations by WKB-type method

Violaine Dalmas, Gérard Robert, Gildas Besançon, Didier Georges

Abstract— **Exact analytical solutions of linearized Saint-Venant equations remain unknown except for uniform regime but this later configuration is not often encountered in real open-channel hydraulic system. In this paper, an approximate solution of linearized Saint-Venant equations in their general non-uniform shape is proposed. This solution is based on a mathematical method developed in quantum mechanics to handle differential equations with space-varying coefficients. It results in irrational transfer functions between levels or flows and boundary flows at any point of the channel and it captures all resonance modes. The accuracy of the method is illustrated on a case study.**

Index Terms— **Open-channel system, Saint-Venant equations, Irrational modeling, WKB method.**

I. Introduction

A. Motivations

Saint-Venant equations [1] are non-linear partial derivatives equations describing water flow. Their linearized form is known to provide an accurate model for open-channel dynamics (see [2]). But no analytical solution is available. Distributed solutions can be found only numerically with appropriate time and space discretizations. As a hydroelectricity producer, EDF (*Électricité de France*) operates run-of-the-river power plants (17.6 TWh produced power per year in France). The power production under environmental respect requires good knowledge, monitoring and control of the water flow along the open-channel. This motivates research on analytical models which can give quantitative information on the dynamics of the flow around operating points. This is useful not only for controller design, but also for civil engineering of the channels.

The literature is abundant concerning analytical models for open-channels. However, except for [3] where a collocation-based model is presented, the majority of publications develop transfer functions which give the water depth dynamics only in the two boundaries. One can find a variety of model type: Integrator Delay [4], Integrator Delay Zero [5], Delay Zero in series with a low-pass filter [6], Integrator Resonance [7]. Notice also that possible resonance modes are not represented by the previous cited models except in [7] where the first resonance mode only is obtained by identification approach. The experiment applied to perform this identification consists in an excitation of the sytem until the oscillating water level shows an increase in amplitude. This type of experiment is not feasible in hydroelectric context where the tidal range is very limited. System identification methods have also been used in [8] and [9] to obtained simplified open-channel models. In the case of [8], a non-resonant open-channel has been considered and the control problem addressed corresponds to long-term hydro-scheduling of the open-channel. No high order dynamic references, such as hydroelectric power generation, are considered. In the case of [9], a fractional-order model is proposed but the high order oscillatory dynamics are not included.

V. Dalmas is with EDF, Hydro Engineering Centre, Savoie Technolac, F-73373 Le Bourget du Lac, France and Univ. Grenoble Alpes, CNRS, Grenoble INP*, GIPSA-lab, 38000 Grenoble, France.

G. Robert is with EDF, Hydro Engineering Centre, Savoie Technolac, F-73373 Le Bourget du Lac, France.

G.Besançon and D.Georges are with Univ. Grenoble Alpes, CNRS, Grenoble INP*, GIPSA-lab, 38000 Grenoble, France.

* Institute of Engineering Univ. Grenoble Alpes

B. Contributions and Outline

In the above context, we propose an approximate analytical solution of linearized Saint-Venant equations *in the general non-uniform regime* based on a so-called *WKB method*. This refers to a mathematical method handling spatially varying coefficients in differential equations which was developed independtly by three physicians G. Wentzel [10], H. A Kramers [11] and L. Brillouin [12] for quantum mechanics study in 1926. It results in a space-dependent solution expressed in Laplace domain, taking the form of irrational transfer functions. They represent with a good accuracy the level-to-flow variations for any operating point, not only at the boundaries, but also at any longitudinal position of a channel. They finally include the resonance modes.

The paper is organized as follows: Saint-Venant equations are introduced in section II. WKB approximation applied to linearized Saint-Venant equation is developed in section III. An illustration is given in section IV before concluding.

II. Saint-Venant equations

A. Non-linear flow model

One-dimensional open-channel flow dynamics are expressed by Saint-Venant equations. They are made of two non-linear hyperbolic partial differential equations in time $t \in \Re^+$ and space $x \in [0; L]$, L being the lenght of the channel. The first one describes the mass conservation; the second one describes the momentum conservation:

$$\begin{cases} \dfrac{\partial S}{\partial t} + \dfrac{\partial Q}{\partial x} = 0 & (1) \\ \dfrac{\partial Q}{\partial t} + \dfrac{\partial (Q^2/S)}{\partial x} + gS\dfrac{\partial H}{\partial x} = gS(I - J). & (2) \end{cases}$$

In the previous system, I is the bottom slope, $H(x,t)$ the water depth, $S(x,t)$ the wetted area, $Q(x,t)$ the discharge, g

the gravity acceleration and J the Manning-Strickler friction slope defined by

$$J = \frac{Q|Q|}{K_s^2 S^2 R_h^{4/3}}, \tag{3}$$

with K_s the Strickler friction coefficient and $R_h(x,t)$ the hydraulic radius. To derive these equations, classical assumptions are made: one-dimensional flow, fluvial regime, uniform cross section, small bed slope, small streamline curvature and negligible vertical acceleration. Furthermore we consider no lateral discharge, nor infiltration.

B. Non-uniform steady state

The previous non-linear partial differential equations (1)-(2) are difficult to use directly for controller design. A first step to reach an effective approximate model is to linearize (1)-(2) around an equilibrium regime in steady state (that is $\partial/\partial t = 0$). In the general case, the equilibrium regime is featured by a stationary state, non-necessarily in uniform regime (i.e. $\partial/\partial x = 0$). Indeed, the open water surface is not necessarily parallel to the channel bottom, as it can be seen on figure 1 where the configuration is typical of a hydroelectric open-channel (see description in section IV). Here we observe a deccelerating profile. In this type of hydroelectric configuration, where the height profile is not only spatially varying but also higher than normal depth, no part of the height profile can be approximated by normal depth. From mass conservation, the equilibrium in Q is necessarily uniform:

$$\frac{dQ_0(x)}{dx} = 0 \Rightarrow Q_0(x) = Q_0 \ constant. \tag{4}$$

From momentum conservation, we derive the depth profile equation as the solution of:

$$\frac{dH_0(x)}{dx} = \frac{I - J_0(x)}{1 - {F_0}^2(x)}, \tag{5}$$

with

$$F_0(x) = \frac{V_0(x)}{c_0(x)} \tag{6}$$

the Froude number corresponding to the ratio between the flow speed $V_0(x) = \frac{Q_0}{S_0(x)}$ and the wave celerity $c_0 = \sqrt{\frac{gS_0(x)}{B_0(x)}}$ with $B_0(x)$ the top width at equilibrium. From (5), one can compute the uniform depth associated to the example described in section IV. At $Q_0 = 1000m^3/s$, one gets $2.75m$. It corresponds to exact compensation of the effect of the slope I by the friction J_0. This configuration is a very particular case not often encountered in reality.

In what follows, linearized Saint-Venant equations are considered, around a *non-uniform* regime verifying (4) and (5). They take the following form:

$$\begin{cases} B_0(x)\dfrac{\partial h(x,t)}{\partial t} + \dfrac{\partial q(x,t)}{\partial x} = 0 & (7) \\ \dfrac{\partial q(x,t)}{\partial t} + 2V_0(x)\dfrac{\partial q(x,t)}{\partial x} + B_0(x)\delta_0(x)\dfrac{\partial h(x,t)}{\partial x} \\ \quad + \beta_0(x)q(x,t) - B_0(x)\gamma_0(x)h(x,t) = 0 & (8) \end{cases}$$

where $q(x,t)$ (respectively $h(x,t)$) represents variations of flow rate (respectively of water depth) around equilibrium value Q_0 (repectively $H_0(x)$) , i.e. :

$$q(x,t) = Q(x,t) - Q_0, \tag{9}$$

$$h(x,t) = H(x,t) - H_0(x) \tag{10}$$

and $\delta_0(x)$, $\beta_0(x)$, $\gamma_0(x)$ are given in the appendix.

We assume that q and h are bounded continuous functions. This ensures existence of Laplace transform of q and h and validity of integral expression of inverse transform. Applying Laplace transform on system (7)-(8), we get:

$$\begin{cases} \dfrac{\partial q(x,s)}{\partial x} + B_0(x)sh(x,s) = 0 & (11) \\ 2V_0(x)\dfrac{\partial q(x,s)}{\partial x} + B_0(x)\delta_0(x)\dfrac{\partial h(x,s)}{\partial x} \\ \quad + \Big(\beta_0(x) + s\Big)q(x,s) - B_0(x)\gamma_0(x)h(x,s) = 0 & (12) \end{cases}$$

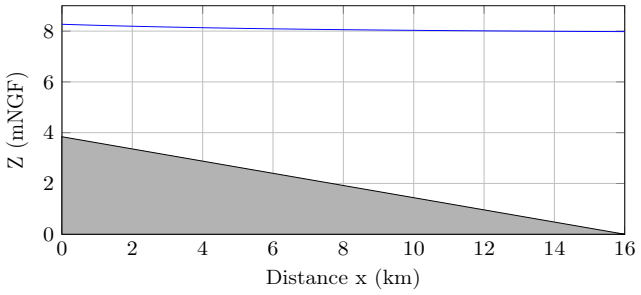

Fig. 1. Backwater curve for $Q_0 = 1000m^3/s, H_0(x = L) = 7.98m$.

Combining the two equations (11)-(12) leads to a second order ordinary differential equation (in short ODE) in flow rate with respect to x:

$$\frac{\partial^2 q(x,s)}{\partial x^2} + M(x,s)\frac{\partial q(x,s)}{\partial x} + N(x,s)q(x,s) = 0 \tag{13}$$

with

$$M(x,s) = -\frac{2V_0(x)s + \rho_0(x)}{\delta_0(x)}, \tag{14}$$

$$N(x,s) = -\frac{s^2 + \beta_0(x)s}{\delta_0(x)}, \tag{15}$$

and $\rho_0(x)$ given in the appendix. One can introduce the controlled boundary conditions at $x = 0$ and $x = L$:

$$q(x = 0, s) = q_{in}(s), \quad q(x = L, s) = q_{out}(s). \tag{16}$$

In what follows, we call *flow rate transfer functions* the discharges-to-flow-rate relations $H_{in}(x,s) := q(x,s)/q_{in}(s)$, $H_{out}(x,s) := q(x,s)/q_{out}(s)$ and *height transfer functions* the discharges-to-height relations $G_{in}(x,s) := h(x,s)/q_{in}(s)$, $G_{out}(x,s) := h(x,s)/q_{out}(s)$.

For the case of uniforme regime, one can handle (13) analytically. All coefficients in (13) are constant and the solution is known (see [13]). In the case of *non-uniform* regime, space-dependent coefficients $M(x,s)$ and $N(x,s)$ are significantly varying, as illustrated on figure 2 for numerical values of the first example presented in section IV.

This means that a special care is to be paid to this space-varying case, and thus we propose an appropriate method in next section.

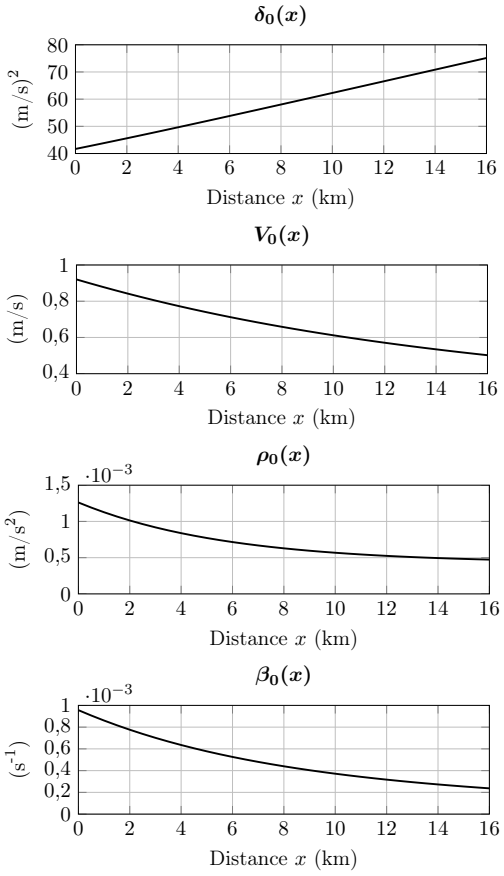

Fig. 2. Coefficients of second order ODE (13).

III. WKB METHOD FOR HYDRAULIC OPEN-CHANNEL

A. framework

Let us consider an equation of the form:

$$\frac{\partial^2 w(x,s)}{\partial x^2} + r(x,s)w(x,s) = 0 \tag{17}$$

where $r(x,s)$ is a slowly varying function of x. Equation (17) can be solved analytically only for constant r or for specific form of r function. Otherwise, no analytical solution is known. WKB method is based on an ansatz on the form of the solutions of (17) for any slowly varying function r in x. It assumes two particular linearly independent solutions of the form

$$\hat{w}_{\pm}(x,s) = A(x,s)e^{\pm j\phi(x,s)} \tag{18}$$

where A and ϕ are the new two unknown functions to be found.

In the context of quantum mechanics [14], A and ϕ are univariate and real, and they are identified by separation of (17) into real and imaginary parts. We can show that in our case where these terms depend on complex Laplace variable s, the separation is the same, leading to two differential equations. After computation we get that $A(x,s)$ and $\phi(x,s)$ are solutions of the system:

$$\begin{cases} \dfrac{\partial^2 A(x,s)}{\partial x^2} - A(x,s)\Big(\dfrac{\partial \phi(x,s)}{\partial x}\Big)^2 = -r(x,s)A(x,s) & (19) \\ A(x,s)\dfrac{\partial^2 \phi}{\partial x^2} + 2\dfrac{\partial A(x,s)}{\partial x}\dfrac{\partial \phi(x,s)}{\partial x} = 0 & (20) \end{cases}$$

1) Computation of the approximate phase from equation (19)*:*
Equation (19) cannot be solved analytically in general because of non-uniformity introduced by $r(x,s)$. The exact solution is known if $r(x,s)$ is constant which is not the case in general. Thus, to deal with the non-uniform case, we make an approximation. Let's rewrite (19) as follows:

$$\frac{1}{A(x,s)}\frac{\partial^2 A(x,s)}{\partial x^2} + r(x,s) - \Big(\frac{\partial \phi}{\partial x}\Big)^2 = 0 \tag{21}$$

Solving equation (21) is a very difficult problem. But it becomes independent of $A(x,s)$ by neglecting the term $\dfrac{\partial^2 A(x,s)}{\partial x^2}\Big/A(x,s)$ with regards to $r(x,s)$. This amounts to assume that the amplitude change is far more slower than the amplitude itself. We make this approximation leading to:

$$\frac{\partial \phi(x,s)}{\partial x} = \pm\sqrt{r(x,s)}. \tag{22}$$

Its solution is

$$\boxed{\phi(x,s) = \pm\int_0^x \sqrt{r(x',s)}dx' + \phi_0} \tag{23}$$

where ϕ_0 is the constant of integration.

2) Computation of the approximate amplitude from equation (20)*:*
By assuming $A(x,s) \neq 0$, equation (20) can be re-written as

$$\frac{1}{A(x,s)}.\frac{\partial}{\partial x}\Big(A^2(x,s)\frac{\partial \phi(x,s)}{\partial x}\Big) = 0 \tag{24}$$

and thus we get $A^2(x,s)\frac{\partial \phi(x,s)}{\partial x}$ constant. Therefore, the amplitude can be written as

$$A(x,s) = \frac{C(s)}{\sqrt{\frac{\partial \phi(x,s)}{\partial x}}} \tag{25}$$

with $C(s)$ a constant in x. Using the expression of $\phi(x,s)$ identified in (23), the amplitude (25) can be explicitely expressed in $r(x,s)$:

$$\boxed{A(x,s) = \frac{C(s)}{\Big(r(x,s)\Big)^{1/4}}}. \tag{26}$$

B. WKB formulation for Saint-Venant equations

ODE (13) under boundary conditions (16) is a boundary-value problem. We look for the existence and unicity of a solution for such a boundary-value problem. It is guaranteed under a generalization of the Wronskian condition [15]: If $q_1(x)$ and $q_2(x)$ are two linearly independent solutions of the differential equation (13), then the general solution can

be written as $q(x,s) = C_1(s)q_1(x,s) + C_2(s)q_2(x,s)$. The boundary conditions require that

$$C_1(s)q_1(x=0,s) + C_2(s)q_2(x=0,s) = q_{in}(s), \quad (27)$$
$$C_1(s)q_1(x=L,s) + C_2(s)q_2(x=L,s) = q_{out}(s). \quad (28)$$

These equations can be solved for unique $C_1(s)$ and $C_2(s)$ in terms of $q_{in}(s)$ and $q_{out}(s)$, provided that

$$\det \begin{vmatrix} q_1(x=0,s) & q_2(x=0,s) \\ q_1(x=L,s) & q_2(x=L,s) \end{vmatrix} \neq 0 \ . \quad (29)$$

$\Big(q_1(x=0,s)q_2(x=L,s) - q_1(x=L,s)q_2(x=0,s) = 0\Big)$ corresponds to an ill-posed problem where there would be no solution or an infinite number of solutions. Otherwise, we have unique $H_{in}(x,s),\ H_{out}(x,s)$ such that:

$$q(x,s) = H_{in}(x,s)q_{in}(s) + H_{out}(x,s)q_{out}(s) \quad (30)$$

Let us consider the following change of variable:

$$w(x,s) = q(x,s)e^{-S(0,x,s)} \quad (31)$$

with

$$S(x_1,x_2,s) = S_1(x_1,x_2)s + S_0(x_1,x_2), \quad (32)$$
$$S_1(x_1,x_2) = \int_{x_1}^{x_2} \frac{V_0(x)}{\delta_0(x)}dx, \quad (33)$$
$$S_0(x_1,x_2) = \frac{1}{2}\int_{x_1}^{x_2} \frac{\rho_0(x)}{\delta_0(x)}dx. \quad (34)$$

Then ODE (13) can be re-written with only second derivative and non-derivative terms as

$$\frac{\partial^2 w(x,s)}{\partial x^2} + r(x,s)w(x,s) = 0 \quad (35)$$

with

$$r(x,s) = -\Big(r_2(x)s^2 + r_1(x)s + r_0(x)\Big) \quad (36)$$

and

$$r_2(x) = \Big(\frac{c_o(x)}{\delta_0(x)}\Big)^2 \quad (37)$$
$$r_1(x) = \frac{\beta_0(x)}{\delta_0(x)} - \frac{d}{dx}\Big(\frac{V_0(x)}{\delta_0(x)}\Big) + \frac{V_0(x)\rho_0(x)}{{\delta_0}^2(x)} \quad (38)$$
$$r_0(x) = -\frac{1}{2}\frac{d}{dx}\Big(\frac{\rho_0(x)}{\delta_0(x)}\Big) + \frac{1}{4}\Big(\frac{\rho_0(x)}{\delta_0(x)}\Big)^2. \quad (39)$$

1) General approximate solution:
The Wronskian condition (29) with the two particular approximate solutions corresponds to

$$A(0,s)A(L,s)e^{\phi(0,s)-\phi(L,s)}\left(1 - \frac{1}{e^{\phi(0,s)-\phi(L,s)}}\right) \neq 0 \quad (40)$$

which satisfies condition (29). Finally $\hat{w}(x,s)$ can be written as

$$\hat{w}(x,s) = \frac{C_1(s)}{\big(r(x,s)\big)^{1/4}}e^{jR(0,x,s)} + \frac{C_2(s)}{\big(r(x,s)\big)^{1/4}}e^{-jR(0,x,s)} \quad (41)$$

with $\phi_0,\ C(s)$ absorbed into $C_1(s)$ and $C_2(s)$ to be determined according to boundary conditions and

$$R(x_1,x_2,s) = \int_{x_1}^{x_2} \sqrt{r(x,s)}dx. \quad (42)$$

2) Derivation of irrational transfer functions:
After computation, we get

$$C_1(s) = \frac{r^{1/4}(0,s)e^{-jR(0,L,s)}q_{in}(s) - r^{1/4}(L,s)e^{-S(0,L,s)}q_{out}(s)}{e^{-jR(0,L,s)} - e^{jR(0,L,s)}}, \quad (43)$$
$$C_2(s) = \frac{-r^{1/4}(0,s)e^{jR(0,L,s)}q_{in}(s) + r^{1/4}(L,s)e^{-S(0,L,s)}q_{out}(s)}{e^{-jR(0,L,s)} - e^{jR(0,L,s)}}. \quad (44)$$

The final expressions of the WKB-approximate flow rate transfer functions after computations of boundaries constants in $q_{in}(s)$ and $q_{out}(s)$ are

$$\boxed{\widehat{H}_{in}(x,s) = \frac{\sin(R(x,L,s))}{\sin(R(0,L,s))}\Big(\frac{r(0,s)}{r(x,s)}\Big)^{1/4}e^{S(0,x,s)}} \quad (45)$$

$$\boxed{\widehat{H}_{out}(x,s) = \frac{\sin(R(0,x,s))}{\sin(R(0,L,s))}\Big(\frac{r(L,s)}{r(x,s)}\Big)^{1/4}e^{-S(x,L,s)}} \quad (46)$$

with $r(x,s)$ given in (36) and $S(0,x,s)$ given in (32). It can be shown that in uniform regime (with constant coefficients), these transfer functions reduce to the exact analytical ones that can be found in [13].

The final expressions of the WKB-approximate height transfer functions are computed from flow rate models $\widehat{H}_{in}, \widehat{H}_{out}$ and from mass conservation equation. We get the height transfer functions:

$$\boxed{\widehat{G}_{in}(x,s) = -\frac{1}{B_0(x)s}\frac{\partial \widehat{H}_{in}(x,s)}{\partial x}}, \quad (47)$$

$$\boxed{\widehat{G}_{out}(x,s) = -\frac{1}{B_0(x)s}\frac{\partial \widehat{H}_{out}(x,s)}{\partial x}}. \quad (48)$$

IV. Illustration

In order to illustrate the approximation performance of models (47) and (48), let us consider a case study of an open-channel with numerical data given in table I.

TABLE I
Open-channel setting

Channel length	$L(km)$	16
Longitudinal coordinate	$x(km)$	12
Bed width	$b(m)$	240
Side angle	$\alpha(deg)$	69
Bed slope	I	$2.4e^{-4}$
Strickler coefficient	$K_s(m^{1/3}/s)$	50
Uniform flow	$Q_0(m^3/s)$	1000
Downstream water depth	$H_0(m)$	7.98

The reference frequency responses $H_{in}(x,s)$, $H_{out}(x,s)$, $G_{in}(x,s)$ and $G_{out}(x,s)$ can be obtained by injection of the solution of equation (13) into (11). More precisely, by

solving numerically equation (13) one obtains the transfers in frequency domain between $(q_{in}(s), q_{out}(s))$ and $q(x,s)$ for any $x \in [0, L]$. Next, by injecting them in (11), one obtains the transfers between $(q_{in}(s), q_{out}(s))$ and $h(x,s)$. This can be done numerically for instance following the algorithm described in [16]. These numerical transfer functions can be considered as exact frequency responses but their numerical form is useless to draw parametric analysis and control design in a convenient way. Morevover, their obtention is computationally costing.

Bode diagrams of height transfer functions obtained either with WKB method or directly numerically are given in figures 3 and 4 on a frequency range relevant for control. We give the results for an intermediary point of the open-channel at $x = 0.75L$ but models can be obtained at any $x \in [0, L]$.

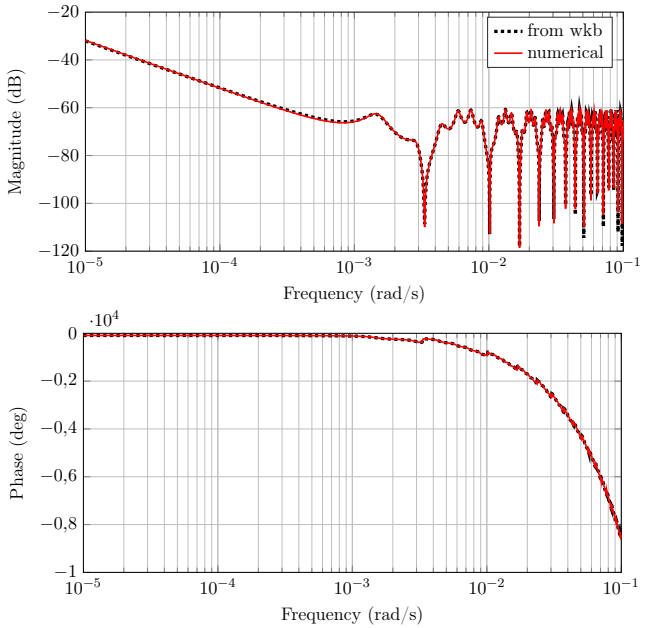

Fig. 3. Bode diagram of $\widehat{G}_{in}(x = 0.75L, s)$ and $G_{in}(x = 0.75L, s)$.

The magnitude plots show a good match. The predominant integrator effect in low frequencies is well captured, and main resonance modes also. The behaviours of the phase plots show that delays are also well represented. The good match can be confirmed by the error plots, given as an illustration for G_{out} in figure 5.

To illustrate the operating point dependency, we choose another configuration of backwater curve for an equilibrium flow of $Q_0 = 500m^3/s$ and an initial steady downstream water depth of $H_0 = 3.98m$. The corresponding normal depth is $1.81m$. The upstream part is close to uniform regime and the downstream part is almost horizontal as one sees on figure 6.

As for the previous example, without approximation of the backwater profile, we apply WKB-type method and show the Bode diagrams on figures 7 and 8 for the intermediary point $x = 0.75L$ represented by a crossmark on figure 6.

Resonances of G_{in} are well captured by the WKB-approximate model also. These eigen modes are periodic due

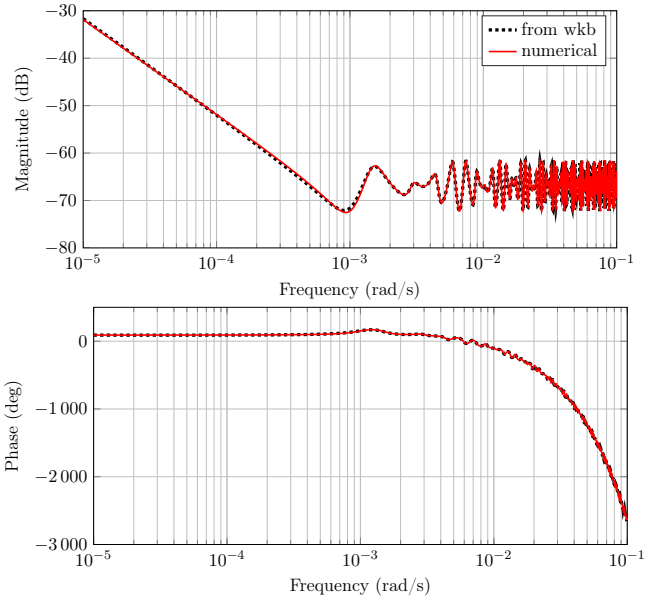

Fig. 4. Bode diagram of $\widehat{G}_{out}(x = 0.75L, s)$ and $G_{out}(x = 0.75L, s)$.

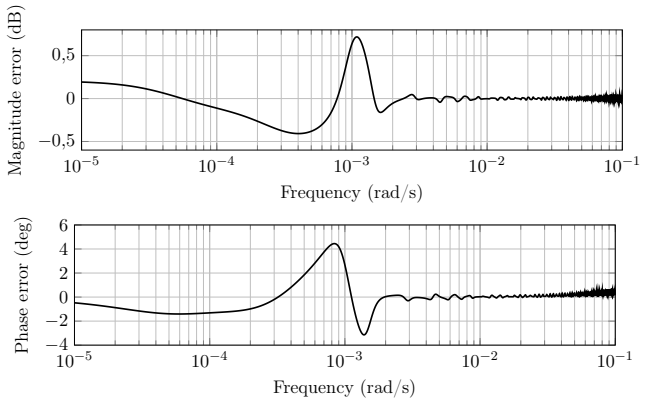

Fig. 5. Errors in magnitude and phase between $\widehat{G}_{out}$ and G_{out}.

to the constant water depth through which they propagate. As expected, G_{out} does not show any resonance mode as they are directly attenuated in the downstream part of the open-channel. By zooming, one can observe some small magnitude modes around the mean high-frequency gain. In this case, a simple IDZ model as proposed in [16] would be convenient for control purpose.

The exact asymptotic low frequency integrator gain is analytically known [16], thus the small steady low frequency error introduced by WKB-method can be corrected in the rationalized approximation step that will be presented in future work.

V. Conclusion

In this paper, an approximate solution of linearized Saint-Venant equations has been proposed from a WKB-type method. The resulting irrational transfer functions include integrator effect, delay and resonance modes. The analytical expression is useful to analyse the dynamic around a non-uniform regime all along the channel. Its possible use for control design will be part of future work. In particular, we

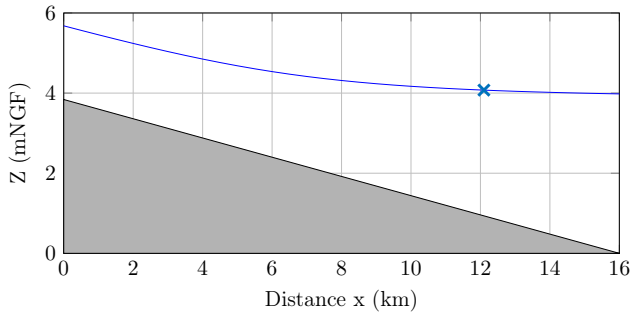

Fig. 6. Backwater curve for $Q_0 = 500m^3/s, H_0(x = L) = 3.98m$.

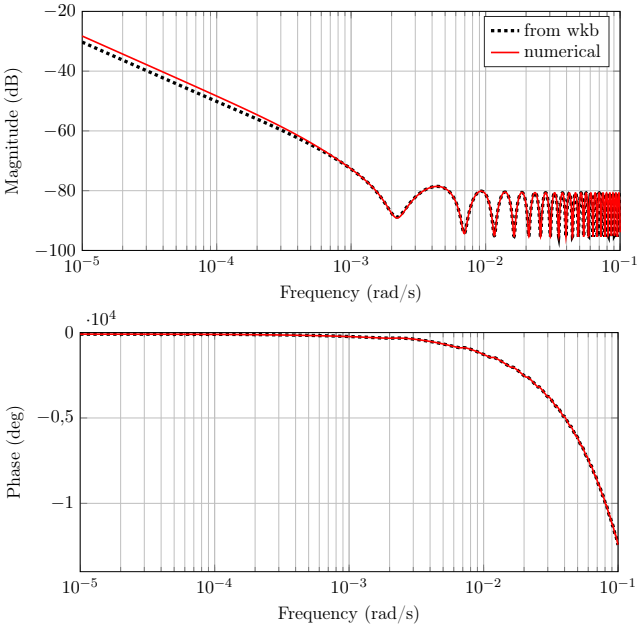

Fig. 7. Bode diagram of $\widehat{G}_{in}(x = 0.75L, s)$ and $G_{in}(x = 0.75L, s)$.

plan to design control law based on rationalized approximation of WKB-type irrational transfer functions. We aim at taking into account the eigen-modes that can be computed from WKB approximate transfer functions.

APPENDIX

Hydraulic coefficients of (7)-(8) are given by

$$\delta_0(x) = {c_0}^2(x) - {V_0}^2(x) \tag{49}$$

$$\beta_0(x) = gS_0(x)J_{0q}(x) + 2\frac{dV_0(x)}{dx} \tag{50}$$

$$\gamma_0(x) = g\left(I - J_0(x) - \frac{dH_0(x)}{dx} - \frac{S_0(x)J_{0h}(x)}{B_0(x)}\right) + \frac{V_0(x)}{B_0(x)}\left(V_0(x)\frac{dB_0(x)}{dx} + 2B_0(x)\frac{dV_0(x)}{dx}\right) \tag{51}$$

with

$$J_{0q}(x) = \frac{2Q_0}{{K_s}^2{S_0}^2(x){R_{h0}}^{4/3}(x)} \tag{52}$$

$$J_{0h}(x) = \left(\frac{2{Q_0}^2{P_0}^{4/3}(x)}{3{K_s}^2{S_0}^{10/3}(x)}\right)\left(\frac{4}{\cos(\alpha)P_0(x)} - \frac{5B_0(x)}{S_0(x)}\right) \tag{53}$$

$$\rho_0(x) = \gamma_0(x) + 2m\frac{\delta_0(x)}{B_0(x)}\frac{dH_0(x)}{dx}. \tag{54}$$

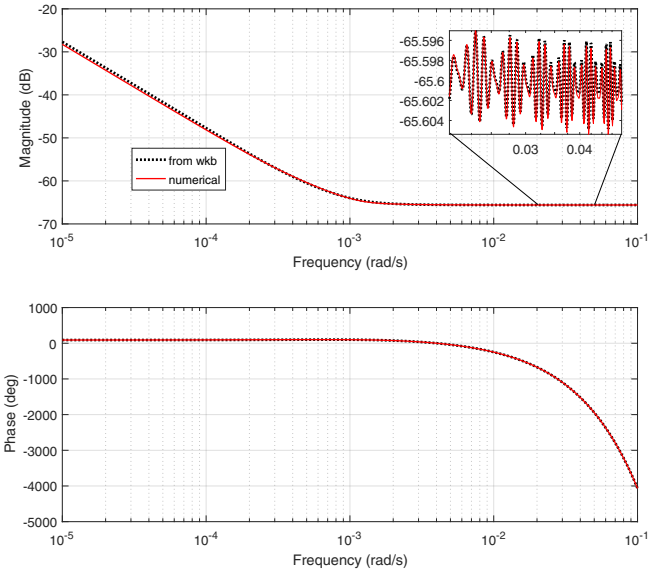

Fig. 8. Bode diagram of $\widehat{G}_{out}(x = 0.75L, s)$ and $G_{out}(x = 0.75L, s)$.

REFERENCES

[1] A. Saint-Venant, *Théorie du mouvement non permament des eaux, avec application aux crues des rivières et à l'introduction de marées dans leurs lits*. Comptes rendus des séances de l'Académie des Sciences, 1871.

[2] V. Chow, *Open-channel Hydraulics*. New-York: McGraw-Hill Book Company, 1959.

[3] J.-F. Dulhoste, G. Besançon, and D. Georges, "Non-linear control of water flow dynamics by input-output linearization based on a collocation model," in *Proceedings of the European Control Conference*, Port, Portugal, July 2001, pp. 2632–2637.

[4] J. Schuurmans, O. Bosgra, and R. Brouwer, "Open-channel flow model approximation for controller design," *Applied Mathematical Modelling*, vol. 19, pp. 525–530, 1995.

[5] X. Litrico and V. Fromion, "Analytical approximation of open-channel flow for controller design," *Applied Mathematical Modelling*, vol. 28, no. 7, pp. 677–695, 2004.

[6] Y. A. Ermolin, "Study of open-channel dynamics as controlled process," *Journal of Hydraulic Engineering*, vol. 118, no. 1, pp. 59–72, 1992.

[7] P.-J. van Overloop, I. J. Miltenburg, X. Bombois, A. J. Clemmens, R. J. Strand, N. C. van de Giesen, and R. Hut, "Identification of resonance waves in open water channels," *Control Engineering Practice*, vol. 18, no. 8, pp. 863–872, 2010.

[8] E. Weyer, "System identification of an open water channel," *Control Engineering Practice*, vol. 9, no. 12, pp. 1289–1299, 2001.

[9] S. N. Calderon-Valdez, V. Feliu-Batlle, and R. Rivas-Perez, "Fractional-order mathematical model of an irrigation main canal pool," *Spanish Journal of Agricultural Research*, vol. 13, no. 3, 2015.

[10] G. Wentzel, "Eine verallgemeinerung der quantenbedingungen fur die zwecke der wellenmechanik," *Zeitschrift fur Physik*, no. 38 (6-7), pp. 518–529, 1926.

[11] A. Kramers, "Wellenmechanik und halbzahlige quantisierung," *Zeitschrift fur Physik*, no. 39 (10-11), pp. 828–840, 1926.

[12] L. Brillouin, "La mécanique ondulatoire de Schrödinger: une méthode générale de résolution par approximations successives," *Comptes Rendus de l'Académie des Sciences.*, no. 183, pp. 24–26, 1926.

[13] V. Dalmas, G. Robert, C. Poussot-Vassal, I. P. Duff, and C. Seren, "From infinite dimensional modelling to parametric reduced-order approximation: Application to open-channel flow for hydroelectricity," in *Proceedings of the European Control Conference*, Aalborg, Denmark, June 2016.

[14] D. J. Griffiths, *Introduction to Quantum Mechanics*. Pearson Education, 2005.

[15] C. Bender and S. Orszag, *Advanced Mathematical Methods for Scientists and Engineers I: Asymptotic Methods and Perturbation Theory*, ser. Advanced Mathematical Methods for Scientists and Engineers. Springer, 1999.

[16] V. Dalmas, G. Robert, G. Besançon, and D. Georges, "Simplified non-uniform models for various flow configurations in open channels," in *Proceedings of the IFAC WC*, Toulouse, France, July 2017.